Development and Validation of MEMS Sun Sensor based on APS detector

Xin Fei, You Zheng

Tsinghua University, Beijing, PRC

2010.8.14

Microsatellite Research in Tsinghua University

Successful Launched

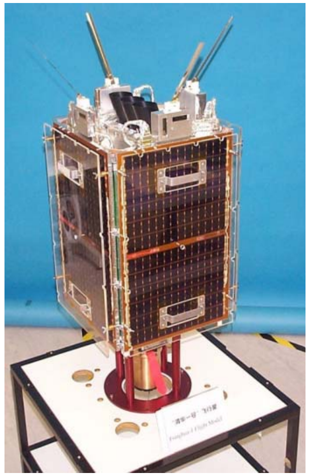

Tsinghua-1

(50kg，2000)

NS-1

(25kg，2004)

Manufactured

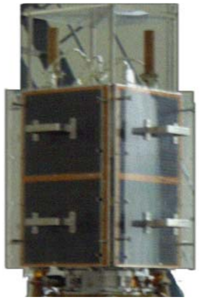

KT-PS
(35kg)

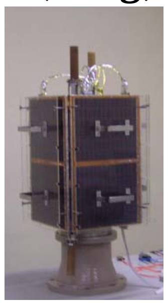

KT-PS1
(35kg)

Waiting for Launch

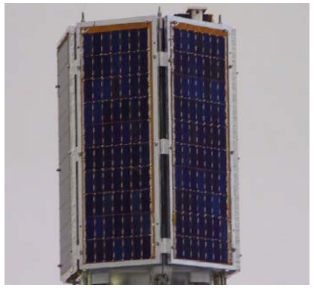

NS-2

(25kg)

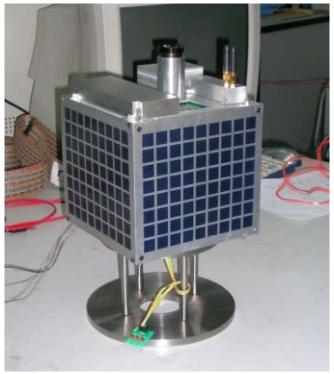

MEMSat

(7kg)

NS-1 is smallest and high density satellite which has been launched in china untill now(or 3 Axis stable smallest satellite in the world)

MEMS device for Space

❑MEMS based Microgyro, Mciroaccelerometor ,Microsunsor, Micromagnetometor, Microthruster, Micro IR sensor, RFdevice and etc.

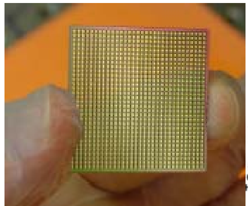

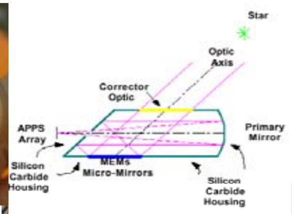

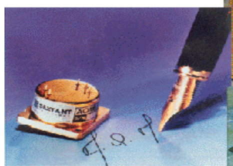

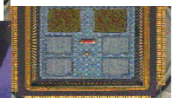

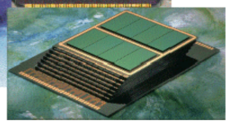

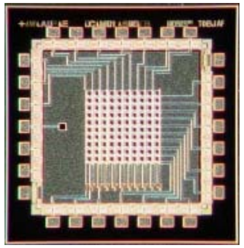

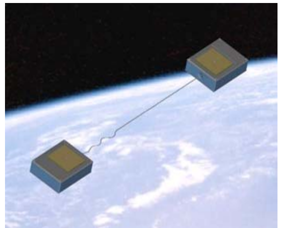

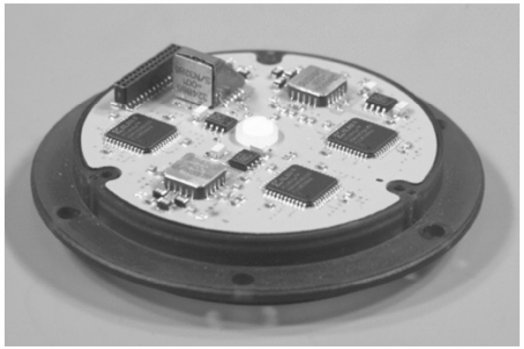

FIGURE 2.7 NMP ST6 ISC MEMS 3-axis gyro assembly. (*Source*: Charles Stark Draper Laboratory.)

❑美国NASA/JPL实验室

Miniature Micro-Navigator

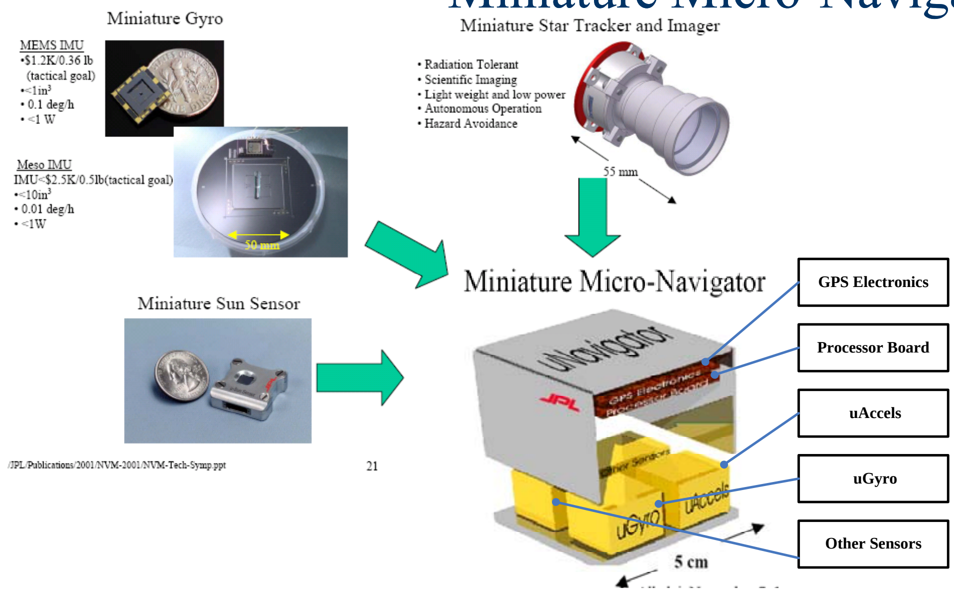

ESA / NASA-JPL / DARPA / ESCC

Topic:

- MNTs flight history and future in-space demonstration
- MNTs programs, trends and roadmaps
- MNTs in space: specific problems and solutions
- New mission concepts and architectures enabled by MNTs
- Systems, subsystems, equipments and devices using MNTs
- MNTs based functioning demonstrators
- Availability & suitability of Micro-Systems Off The Shelf
- Technology transfer to & from other industrial sectors
- Micro-systems design and modelling
- Materials, technologies, foundries & services, packaging
- Micro- machining, rapid prototyping and fabrication
- Testing methods (inc. radiation), procedures & standards
- MNTs Reliability, evaluation and space qualification
- European Strategy for MNTs
- ESA projects and MNTs

Contents

- Introduction
- Engineering Model Construction
- FEIC algorithm
- Performance Validation on lab and orbit
- Summary

Introduction

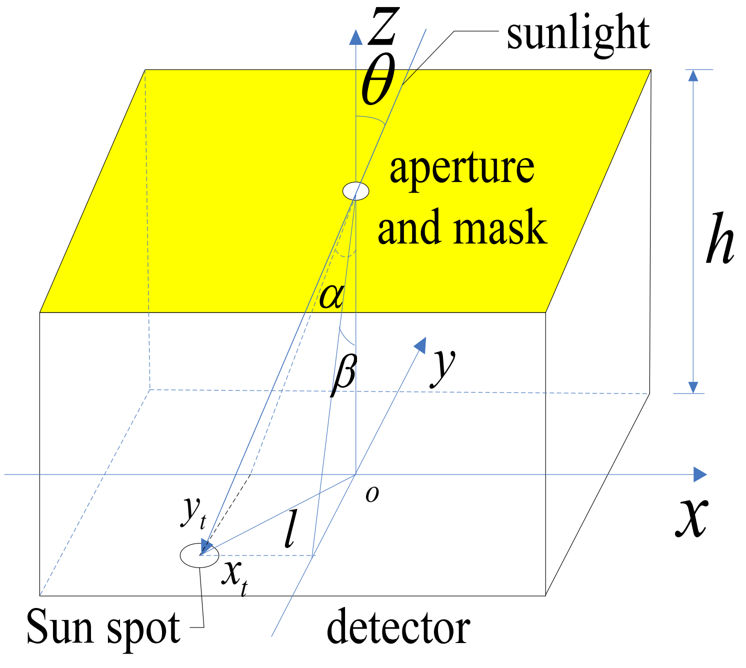

$$\alpha = tg^{-1}\left(\frac{x_c}{h}\right) \qquad \beta = tg^{-1}\left(\frac{y_c}{h}\right)$$

➢Principle

According to the location of sunlight imaging on the detector, determine the incidence angle of sunlight.

➢Construction

1. Optical mask
2. Detector
3. Electricals

Line array(1-D) SS principle

➢Line array principle

Coding format

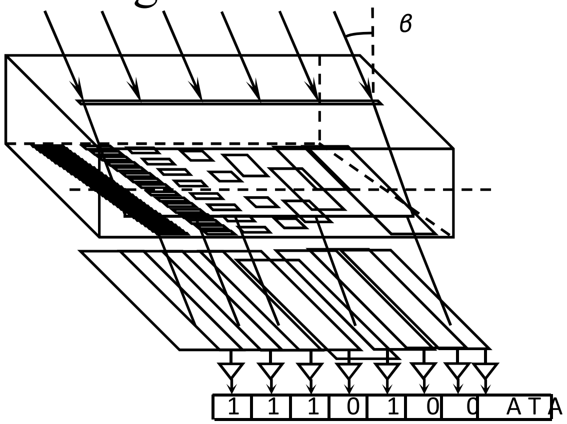

1-D CCD formate

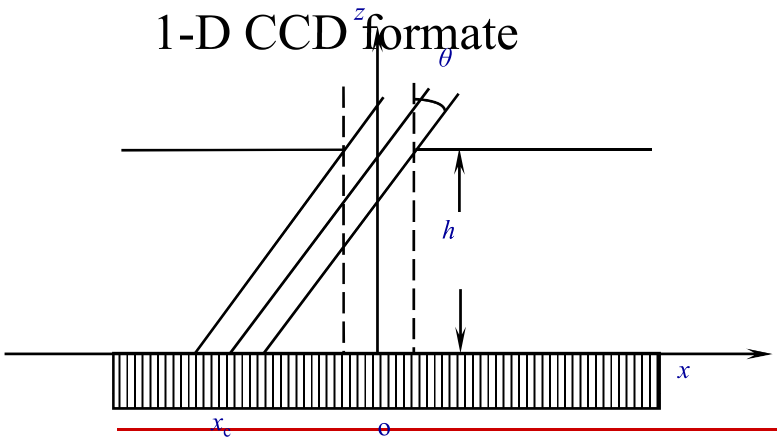

➢prototype

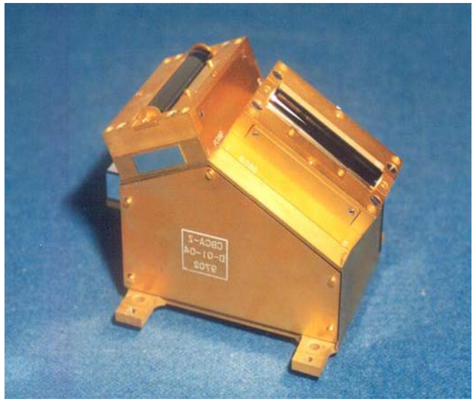

a) DSS2（ China 502）

Area array(2-D) SS principle

➢2-D Principle

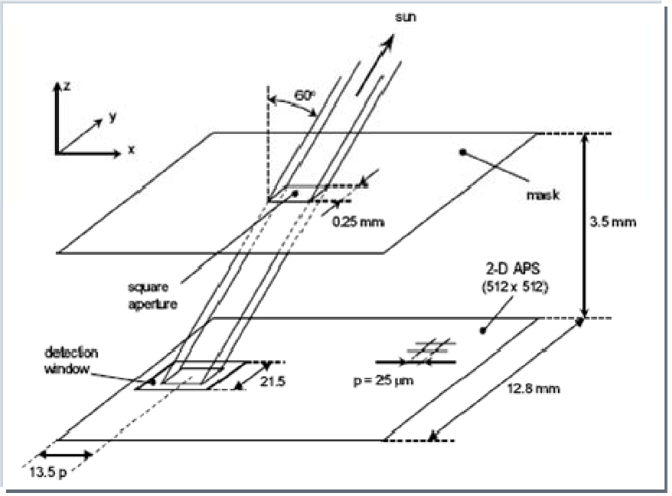

Imaging Principle

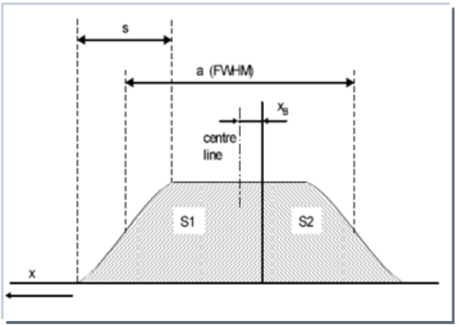

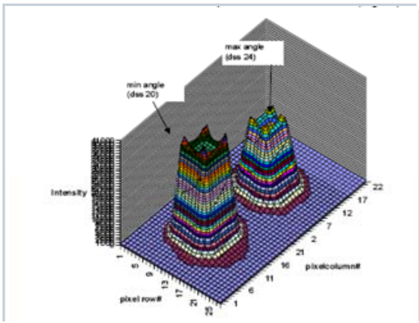

Energy distribution function

➢prototype

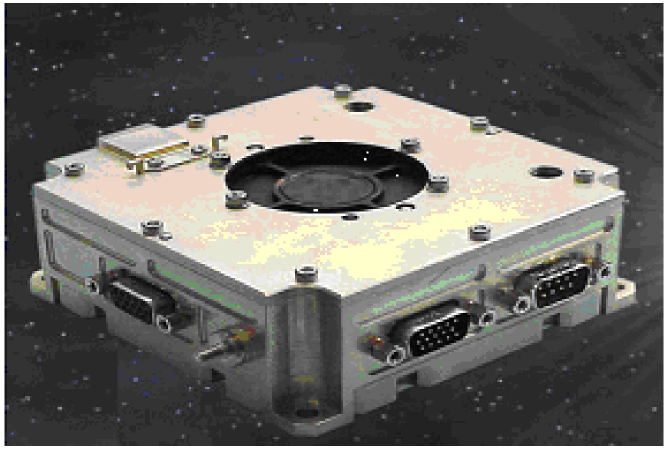

Galileo Corp.（Smart Sun Sensor）

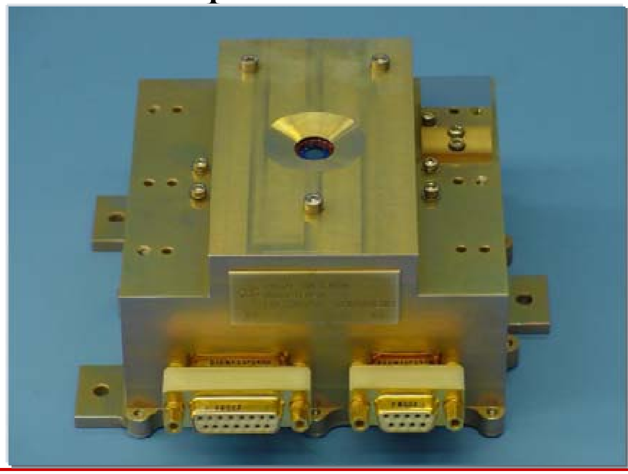

Soldern Corp. DSS

Sun Sensor Trends

- **2-D array instead of line array;**

  improve the accuracy and reliability;

- **APS COMS detector instead of CCD ;**

  improve the space adaptability and speed;

- **Multi-apertures instead of single;**

  improve the accuracy, reliability and robustness.

Contents

- **Introduction**
- **Engineering Model Construction**
- **FEIC algorithm**
- **Performance Validation on lab and orbit**
- **Summary**

System Principle

Construction Principle

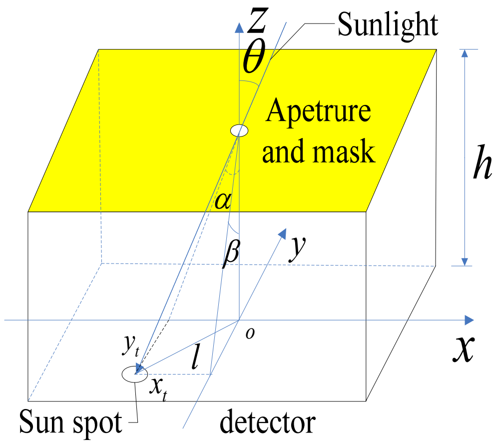

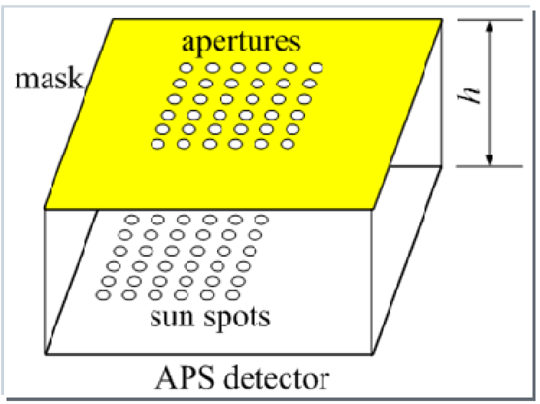

Function Diagram of Sun Sensor

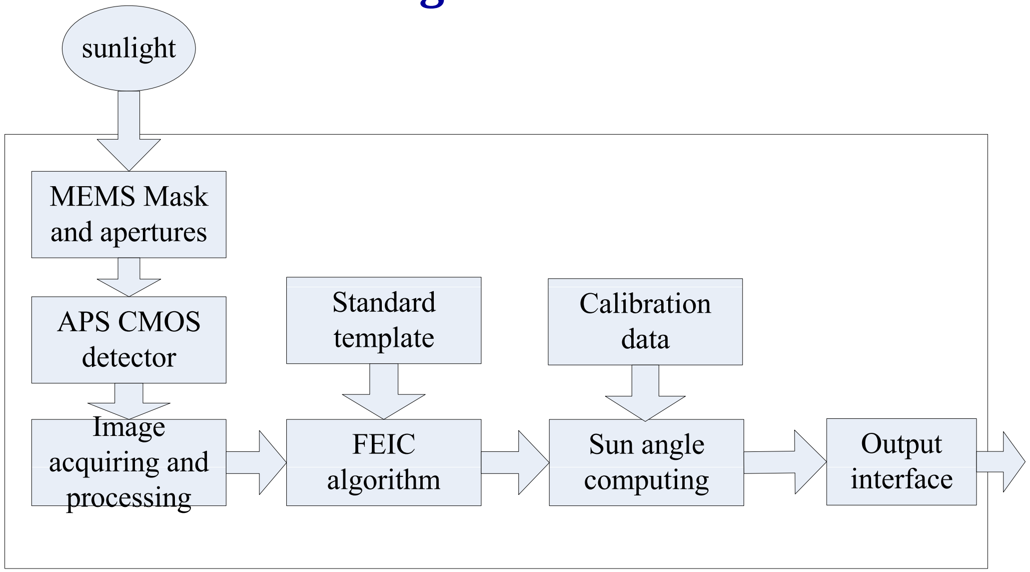

➢Characters

1. **MEMS based apertures array mask**
2. **APS CMOS detectors**
3. **High accurate FEIC algorithm**

Detector Specification

APS CMOS detector

Parameter	Specification
Detector technology	CMOS Active Pixels Sensor
Sensitive area format	1024×1024
Pixel size	15μm×15μm
Spectrum range	400nm～1000nm
Quantum Efficiency ×FF	>20%
Dose Radiation Tolerance	>230krad(si)

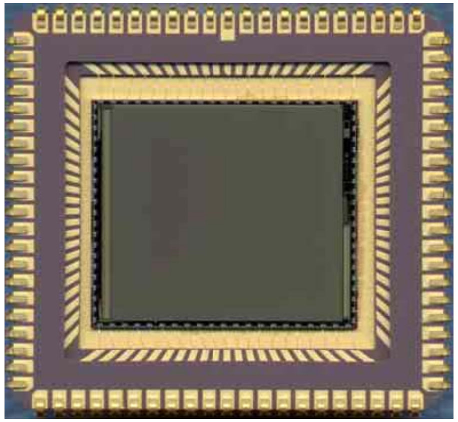

Sunlight tracking route in MEMS sun sensor

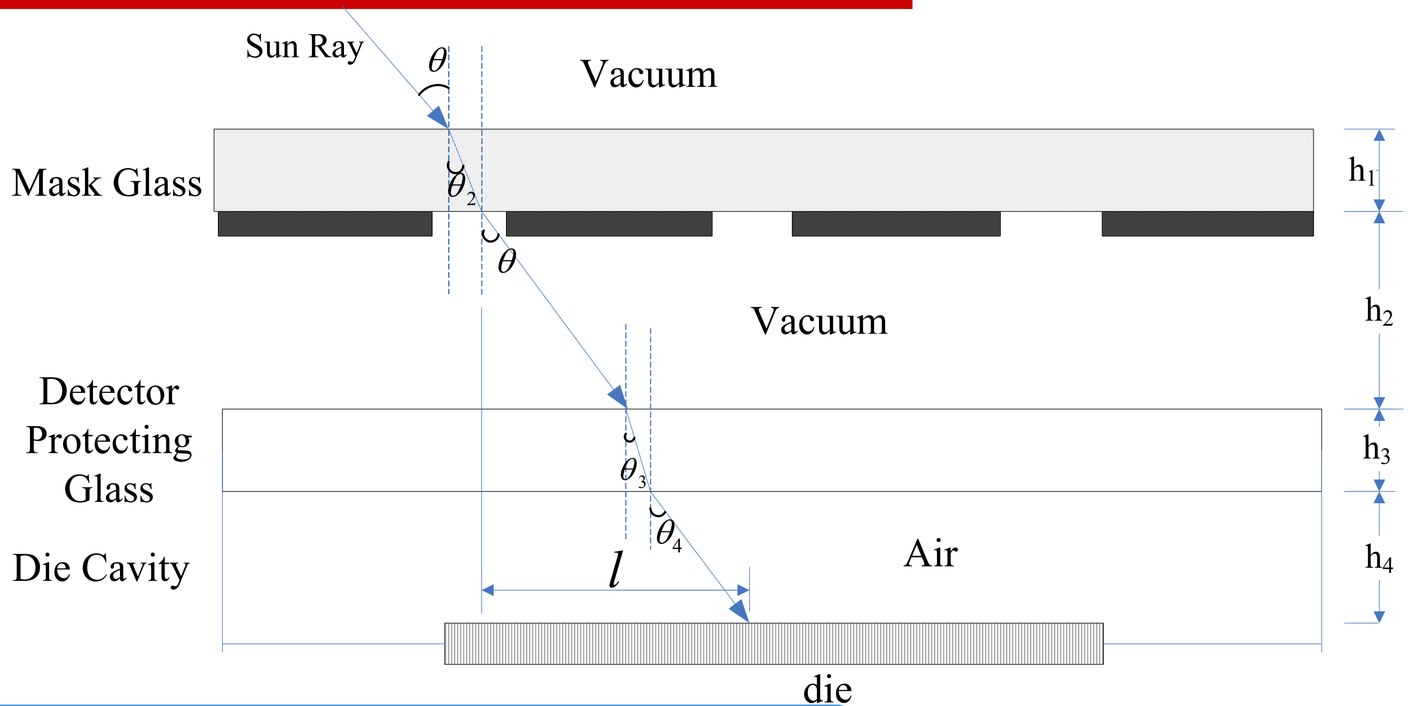

➤Sunlight tracking route

Before Sunlight arriving the detector, it pass through Mask glass, vacuum, Detector protecting glass, Die cavity Air, in turn.

Multi-apertures Mask

➢parameters

1. Radiation Glass thickness : 1.7mm;
2. Apertures format: 6×6;
3. Apertures size 45×45μm^2=3×3 pixels;
4. Apertures distance: 480μm=32pixels;

➢Sketch map

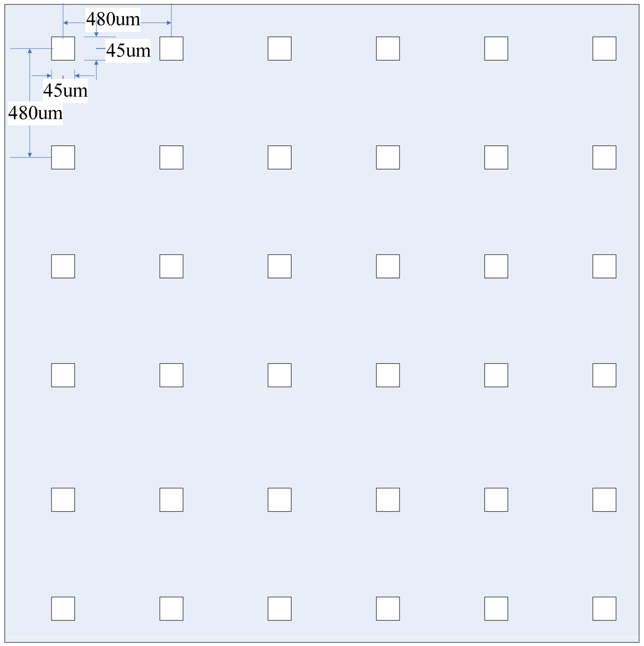

Parameters is determined by accuracy, and rapid capturing and tracking algorithm.

MEMS Processing for mask

Glass Substrate

Sputtering Cr film

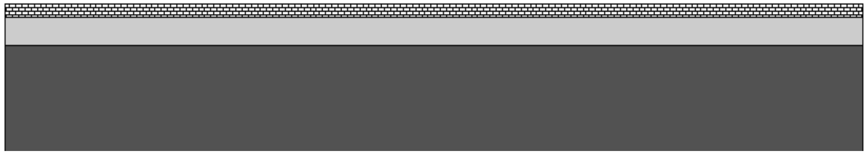

Coating with photoresist

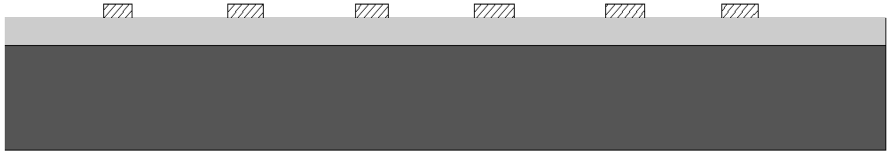

The photoresist patterned lithographically

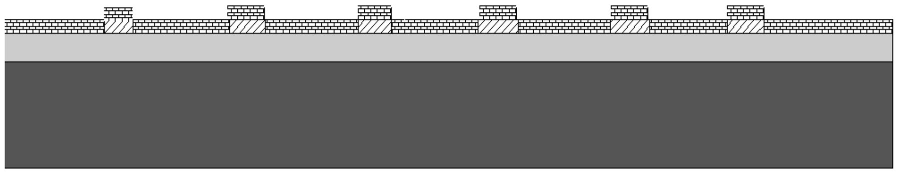

Sputtering Au firstly, then Cr film

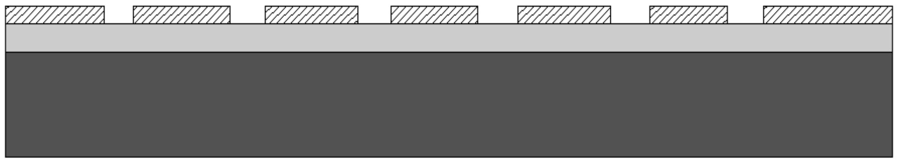

lift-off, forming apertures

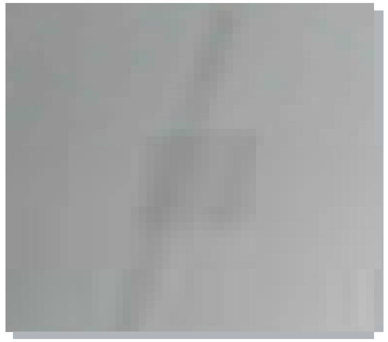

Picture of Mask with 6×6 apertures

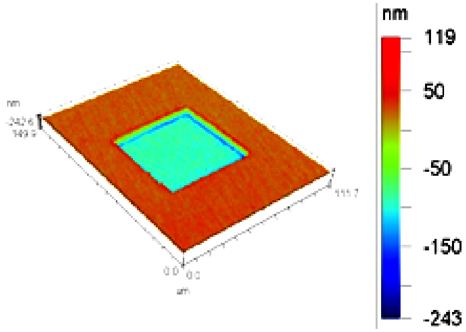

two dimensional surface morphology of the single aperture

Electrics Design

Electrics Sketch map

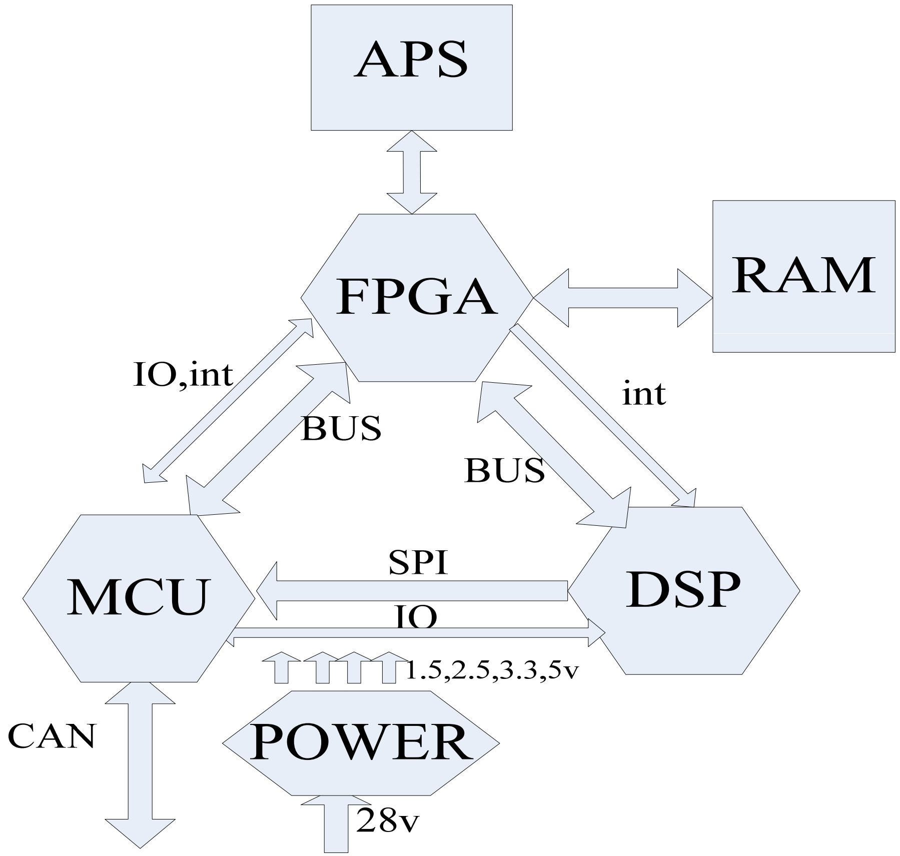

➢Feature

1. **Both DSP and MCU may access the image area via FPGA.**
2. **MCU backups the function of DSP.**

Sun Sensor construction

MEMS based mask

Large array Image sensitivity and readout

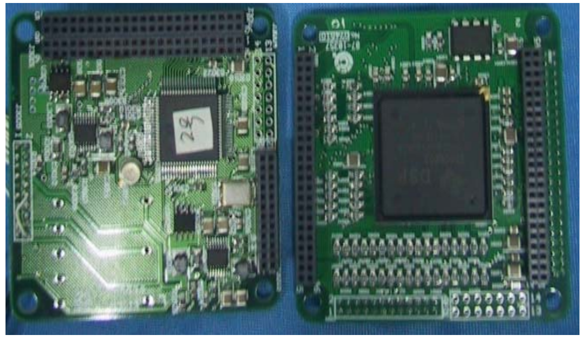

High speed Image processing and attitude computing

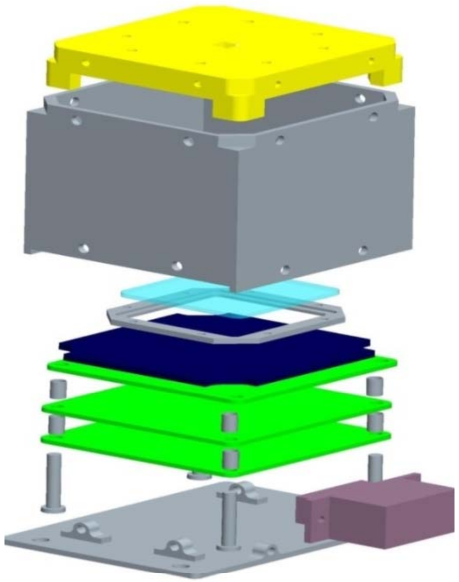

Layers Installation

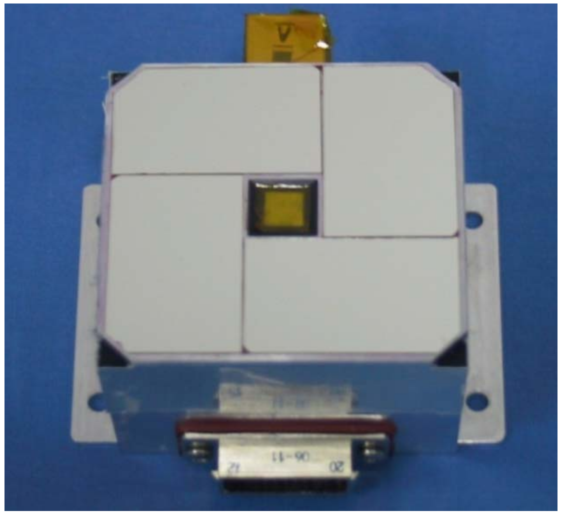

sun sensor Production

Contents

- Introduction
- Engineering Model Construction
- FEIC algorithm
- Performance Validation on lab and orbit
- Summary

Imaging modeling without protected glass

➢Sketch map

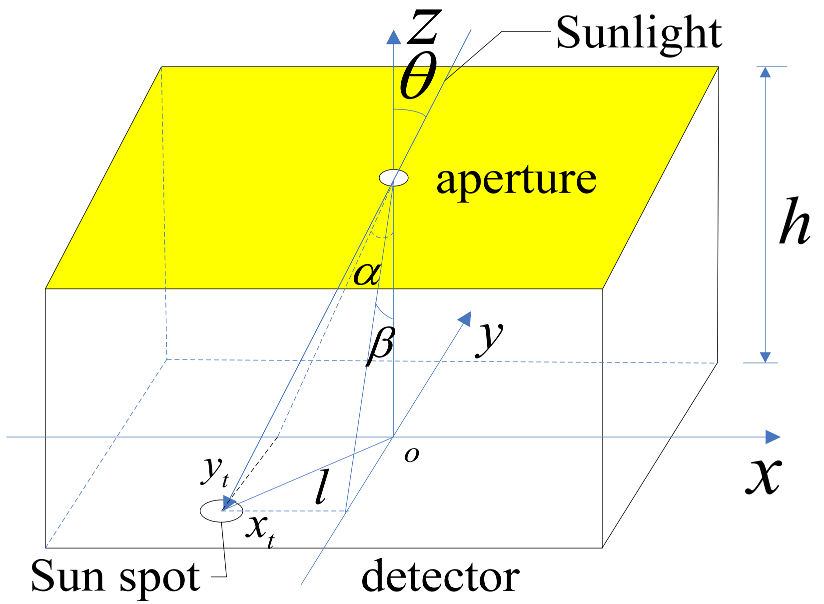

➢equations

$$\theta = \arctan\left(\frac{l}{h}\right), \alpha = \arctan\left(\frac{x_c}{h}\right), \beta = \arctan\left(\frac{y_c}{h}\right) \quad (1)$$

$$l = \sqrt{x_c{}^2 + y_c{}^2} \quad (2)$$

$$\tan\theta = \sqrt{(\tan\alpha)^2 + (\tan\beta)^2} \quad (3)$$

Eq. (1) applies to the case without protected glass ;
Eq. (2),(3) applies to the both case with or without protected glass .

Imaging modeling with protected glass

➢Sketch map

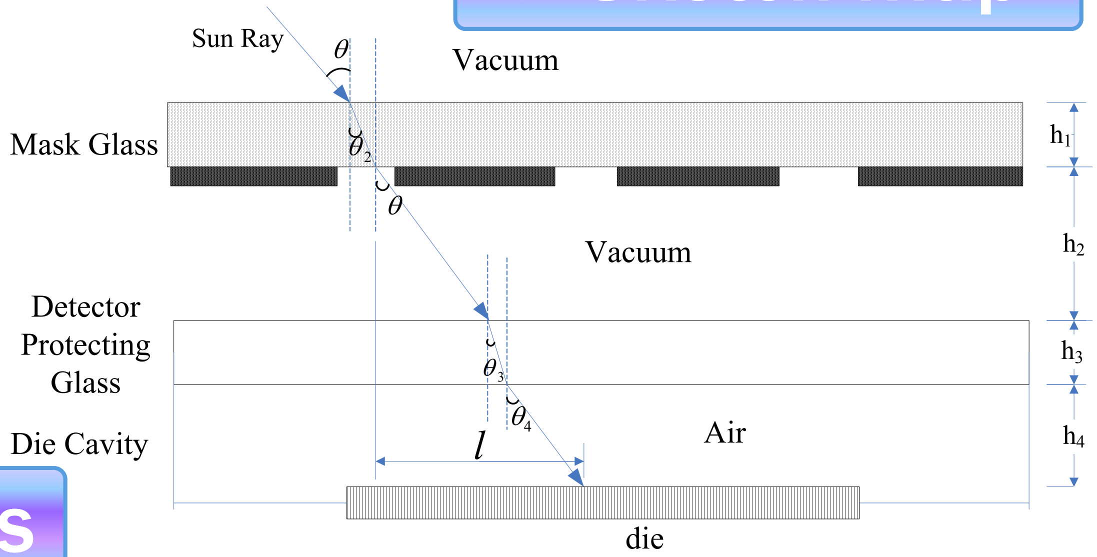

➢equations

$$\theta_2 = \theta$$

$$l = h_2 \tan\theta_2 + h_3 \tan\theta_3 + h_4 \tan\theta_4 \qquad n_3 = \frac{\sin\theta}{\sin\theta_3} \qquad n_4 = \frac{\sin\theta}{\sin\theta_4}$$

Sun spot position l is unrelated with mask glass thickness，and closely related with detector protected glass thickness.

Sun angles computing algorithm with protected glass

➢Function with glass

$$l = h_2 \tan\theta + h_3 \tan\left(\arcsin\left(\frac{\sin\theta}{n_3}\right)\right) + h_4 \tan\left(\arcsin\left(\frac{\sin\theta}{n_4}\right)\right)$$

It is a Monotone function and no analytic solution.

$$\tan\theta = f(l) \qquad l = \sqrt{(x_c - x_0)^2 + (y_c - y_0)^2}$$

$$\tan\theta = \sqrt{(\tan\alpha)^2 + (\tan\beta)^2} = f\left(\sqrt{(x_c - x_0)^2 + (y_c - y_0)^2}\right)$$

➢Key point

$$\alpha = \arctan\frac{-(x_c - x_0)\tan(\theta)}{\sqrt{(x_c - x_0)^2 + (y_c - y_0)^2}}$$

$$\beta = \arctan\frac{-(y_c - y_0)\tan(\theta)}{\sqrt{(x_c - x_0)^2 + (y_c - y_0)^2}}$$

1.The basic idea is through (x_c, y_c) **to solve** $\tan\theta$

2.System accuracy is determined by the accuracy of (x_c, y_c)

MultiApertures image Characteristics

➢Features

1： sun spots only occupy 2% of the whole sensor area；

2： sun spots is equal spacing distribution。

3： the relative position of sun spots in the sensor is invariable, which is design-related, however incident angle.

➢Sun spots

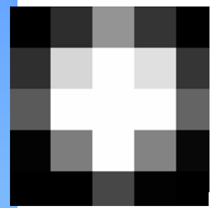

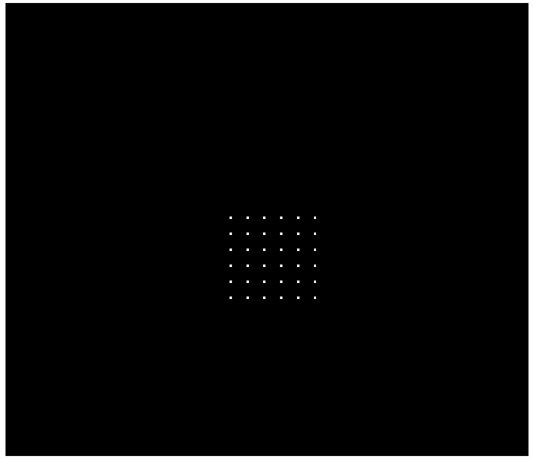

➢Equal spacing distribution model

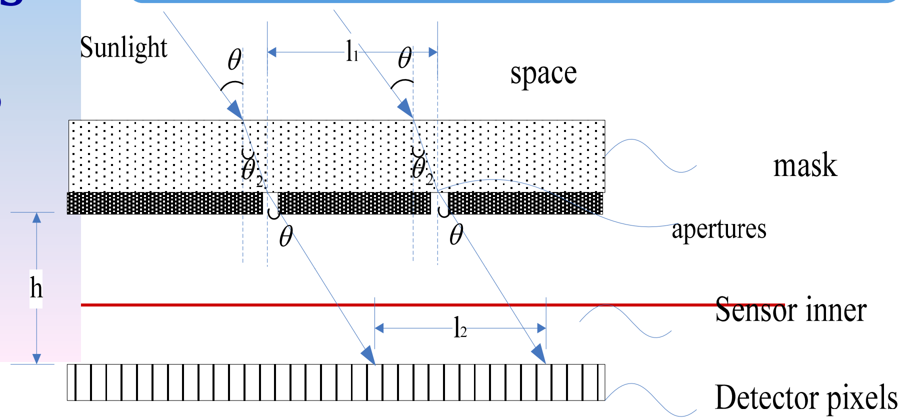

Initial Capturing-templet construction

➢Templet image

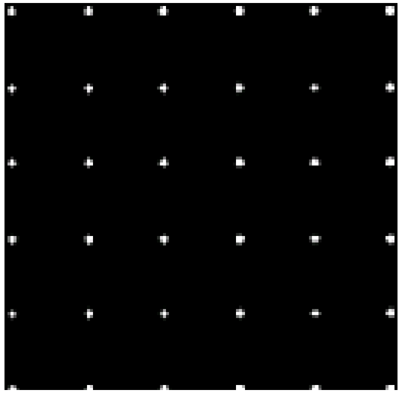

a) Templete image

Features Extraction

1	0	1	0	1	0	1	0	1	0	1	0
0	0	0	0	0	0	0	0	0	0	0	0
1	0	1	0	1	0	1	0	1	0	1	0
0	0	0	0	0	0	0	0	0	0	0	0
1	0	1	0	1	0	1	0	1	0	1	0
0	0	0	0	0	0	0	0	0	0	0	0
1	0	1	0	1	0	1	0	1	0	1	0
0	0	0	0	0	0	0	0	0	0	0	0
1	0	1	0	1	0	1	0	1	0	1	0
0	0	0	0	0	0	0	0	0	0	0	0
1	0	1	0	1	0	1	0	1	0	1	0
0	0	0	0	0	0	0	0	0	0	0	0

b）binary templet

➢Features

Each sun spot signed by 1， circumambience area signend by 0， each 1 enclosued by three 0 constructs one identified area； templet total has 36 identified area.

Initial Capturing-algorithm processing

1. **Image binary storing：** **make Image binarization, and store the binary result pixels every other column and every other row.**

   Image characteristics： **storing binary image meets the 2 bytes and 1024 bytes interval between the horizontal adjacent and vertical adjacent of sun spots.**

1	0	1	0	1	0	1	0	1	0	1	0
0	0	0	0	0	0	0	0	0	0	0	0
1	0	1	0	1	0	1	0	1	0	1	0
0	0	0	0	0	0	0	0	0	0	0	0
1	0	1	0	1	0	1	0	1	0	1	0
0	0	0	0	0	0	0	0	0	0	0	0
1	0	1	0	1	0	1	0	1	0	1	0
0	0	0	0	0	0	0	0	0	0	0	0
1	0	1	0	1	0	1	0	1	0	1	0
0	0	0	0	0	0	0	0	0	0	0	0
1	0	1	0	1	0	1	0	1	0	1	0
0	0	0	0	0	0	0	0	0	0	0	0

⌖ Initial Capturing-algorithm processing

2. **templet：Each sun spot enclosed by 3 dark points, for reliability, at least 31 templets need be recognized.**

$A(i) > 0$ denote that existing a sun spot in the Successive 16 bytes.

$$P(i) = \left(A(i)\ \&\ A(i+1) \right) | \left(A(i)\ \&\ A(i+64\times 8) \right) | \left(A(i)\ \&\ A(i+64\times 8+1) \right)$$

$P(i) = 0$ denote that the sun spot enclosed by dark area.

$$\begin{cases} A(l) > 0 \\ P(l) = 0 \end{cases} \quad l = \{i + k\times 2 + j\times 1024 + p\times 2\} \quad \begin{cases} k = -5, -4, \cdots 0 \\ j = 0, 1, \cdots 5;\ p = 0, 1, \cdots 5 \end{cases}$$

➢Conclusion

To given domain of i, k, if there is l meeting the requirement of $\begin{cases} A(l) > 0 \\ P(l) = 0 \end{cases}$, that indicates the capturing successful.

Future Extraction(FE) Algorithm

➢Sun spots position variation

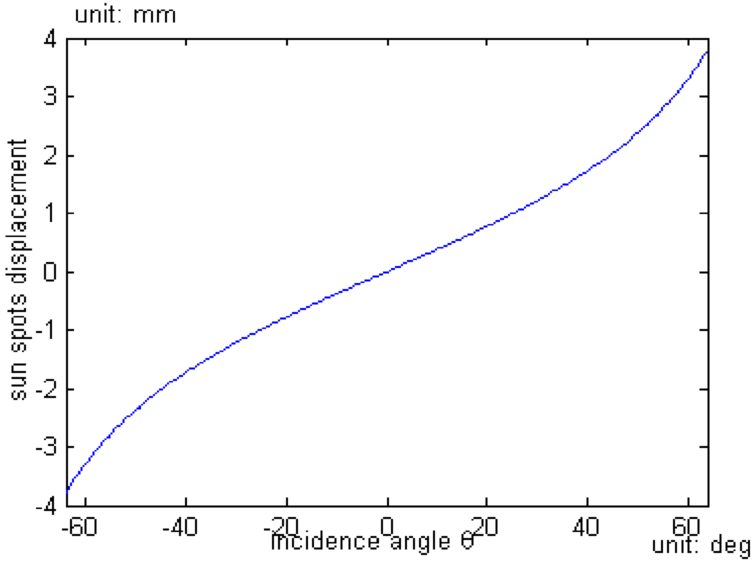

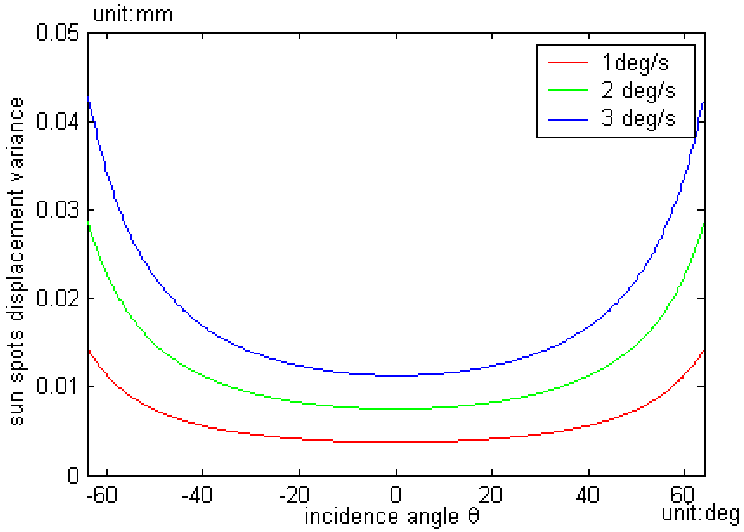

➢characteristics

Sun spots positions have very small change, no more than 4 pixels, between the two successive frames, so the direct recursion is using as the future extraction algorithm.

Future Extraction of APS

➢APS readout

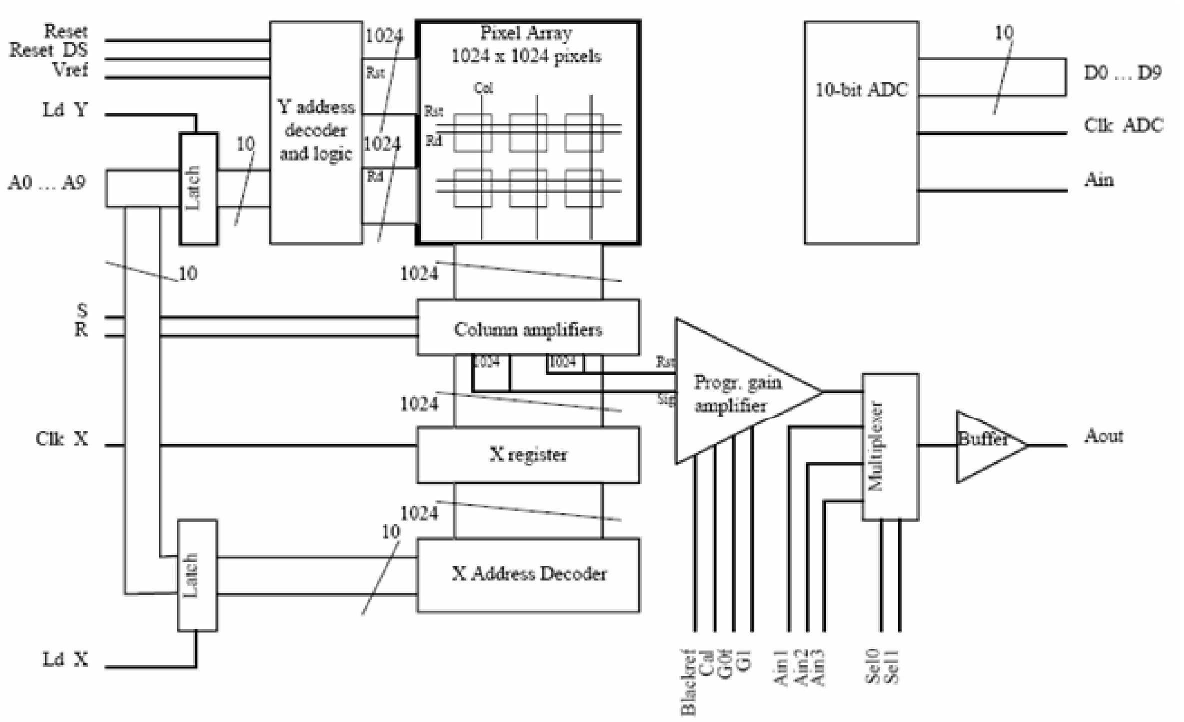

➢Features

APS sensor has multi windows and random access and subsampling functions, with which the FE algorithm can directly image and readout the sun spots region.

image correlation(IC)

➢Sun spot templet

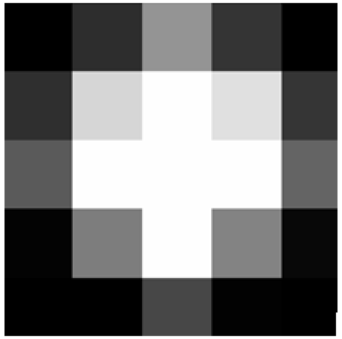

➢Image correlation

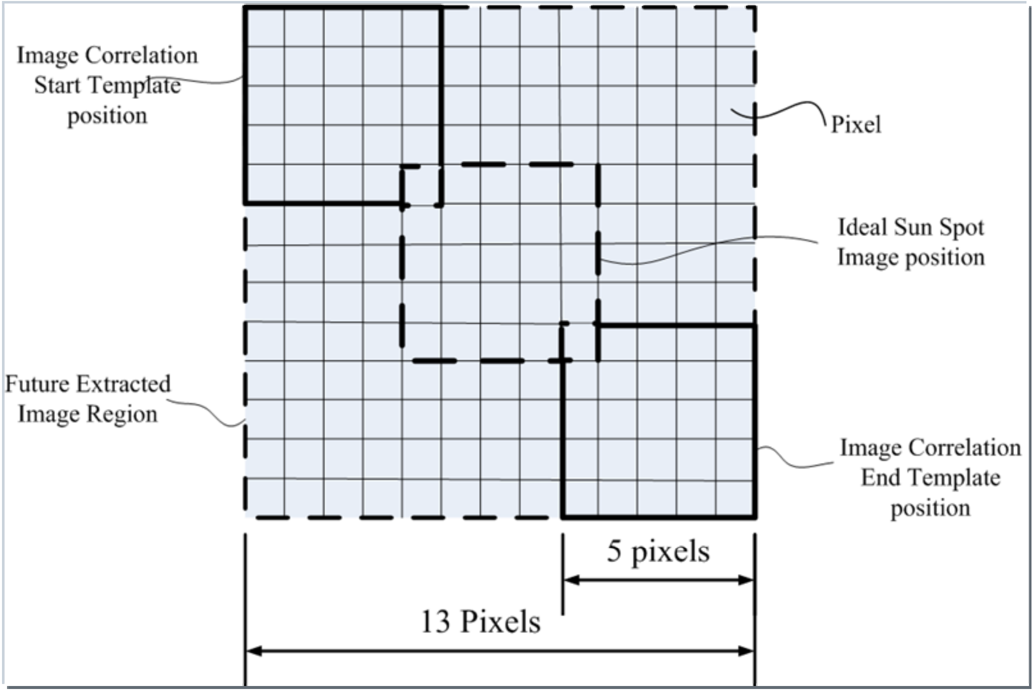

➢FE Sun spot

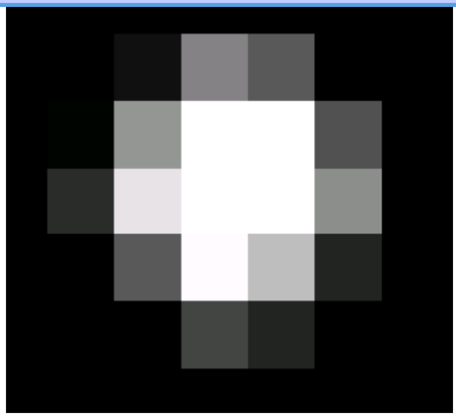

Through the image correlation of the templet and the FE sun spot, acquiring the small change of sun spot position.

Energy distribution after correlation

➢Tradition energy distribution

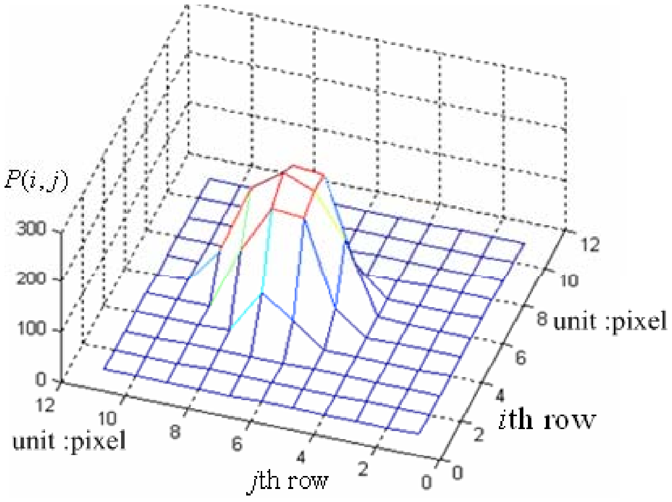

➢energy distribution after IC

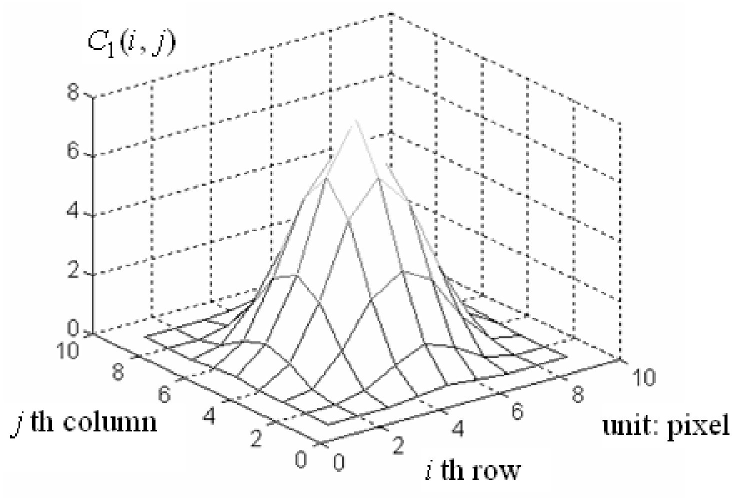

compared to the traditional energy distribution， the sun spot has higher SNR （signal to noise ratio） after IC (image correlation)。

Centroid algorithm after IC

➢Traditional Centroid

$$x_c = \frac{\sum_{i=x_{peak}-k}^{x_{peak}+k} \sum_{j=y_{peak}-k}^{y_{peak}+k} P(i,j) \times i}{\sum_{i=x_{peak}-k}^{x_{peak}+k} \sum_{j=y_{peak}-k}^{y_{peak}+k} P(i,j)}$$

$$y_c = \frac{\sum_{i=x_{peak}-k}^{x_{peak}+k} \sum_{j=y_{peak}-k}^{y_{peak}+k} P(i,j) \times j}{\sum_{i=x_{peak}-k}^{x_{peak}+k} \sum_{j=y_{peak}-k}^{y_{peak}+k} P(i,j)}$$

➢Centroid after IC

$$\tilde{x}_1 = \frac{\sum_{m=0}^{8} \sum_{n=0}^{8} C_1(m,n) \times (m-4)}{\sum_{m=0}^{8} \sum_{n=0}^{8} C_1(m,n)}$$

$$\tilde{y}_1 = \frac{\sum_{m=0}^{8} \sum_{n=0}^{8} C_1(m,n) \times (n-4)}{\sum_{m=0}^{8} \sum_{n=0}^{8} C_1(m,n)}$$

After IC， increasing SNR， degreasing regional pixels impact ， the sun spot location accuracy will be greatly increased.

Multi sun spots weighted algorithm

➢Weighted coefficent

$$x_c = \sum_{i}^{36} a_i x_{ci}$$

$$y_c = \sum_{i}^{36} b_i y_{ci}$$

$$a_i = b_i = \frac{\sum_{m=0}^{8} \sum_{n=0}^{8} C_i(m,n)}{\sum_{i=1}^{36} \sum_{m=0}^{8} \sum_{n=0}^{8} C_i(m,n)}$$

➢Centroid after Weighted

$$x_c = \Delta x + \frac{\sum_{i=1}^{36} \sum_{m=0}^{8} \sum_{n=0}^{8} C_i(m,n)(m-4)}{\sum_{i=1}^{36} \sum_{m=0}^{8} \sum_{n=0}^{8} C_i(m,n)}$$

$$y_c = \Delta y + \frac{\sum_{i=1}^{36} \sum_{m=0}^{8} \sum_{n=0}^{8} C_i(m,n)(n-4)}{\sum_{i=1}^{36} \sum_{m=0}^{8} \sum_{n=0}^{8} C_i(m,n)}$$

➢Features

The energy-weighted method using 36-point not only improves the centroid accuracy better than 0.02 pixels, but also eliminates the impact to system when some the sun spots lost or disturbed.

Solving $\tan\theta$ through polynomial fitting

➢principle

$$l_n = \sqrt{(x_{cn} - x_0)^2 + (y_{cn} - y_0)^2}$$

$$\tan\theta_n = a_5 l_n^5 + a_4 l_n^4 + a_3 l_n^3 + a_2 l_n^2 + a_1 l_n^1 + a_0$$

➢method

To any θ at given axis, measuring the corresponding sun spots position , l acquire the polynomial coefficients。

➢equipments

Sun simulator, two-axis gimbal, Theodolite etc.

Contents

⌖The accuracy performance

Sun sensor in test set-up

Measurement error statistics

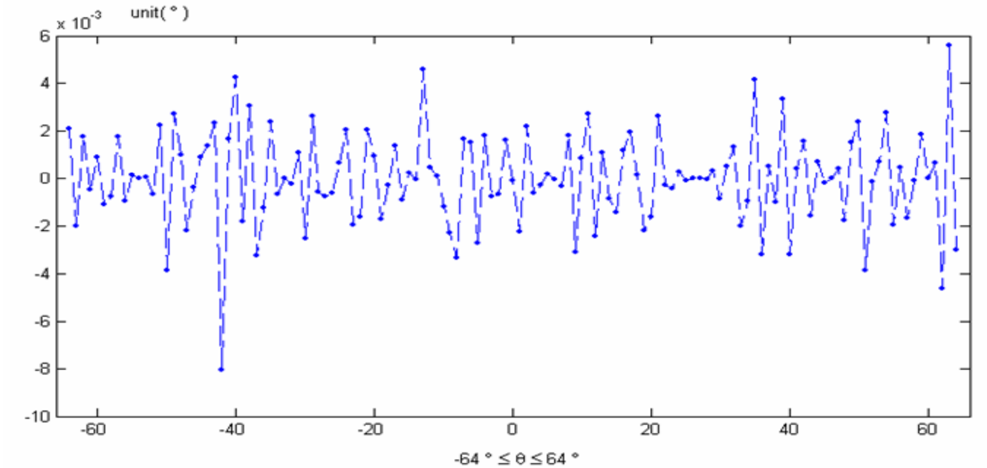

Sensor angle of incidence(°)

➢conclusion

The residual random error is **0.008** degree of arc.

⌖Real sun experiment

Real sun experiment set-up

Sensor output result(Earth's rotation)

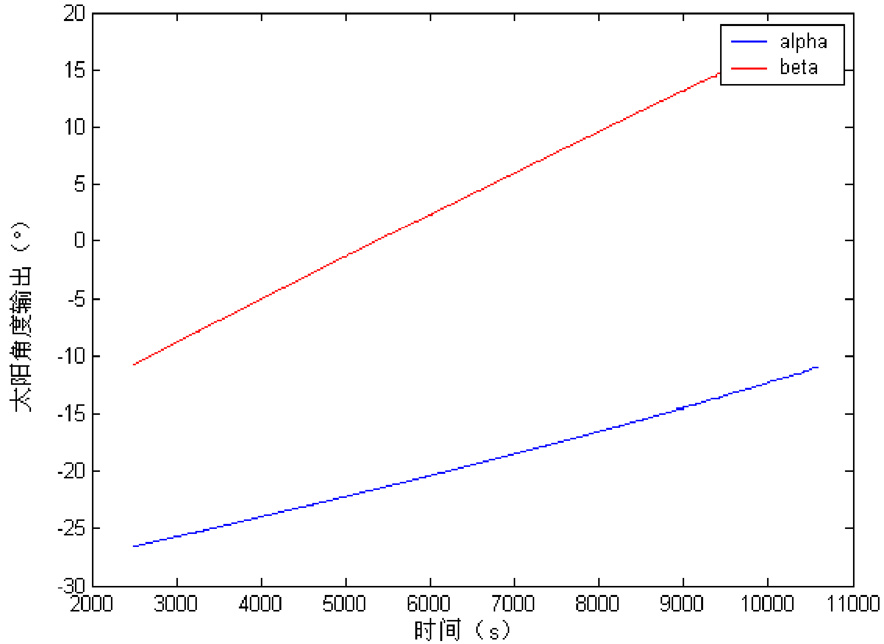

➢conclusion

Sun sensor output data is homologous to (ascending or descending) per second , and no jitter case, which determine that the system resolution of better than 0.004 。

⌖Immunity performance(1)

1： some apertures missing

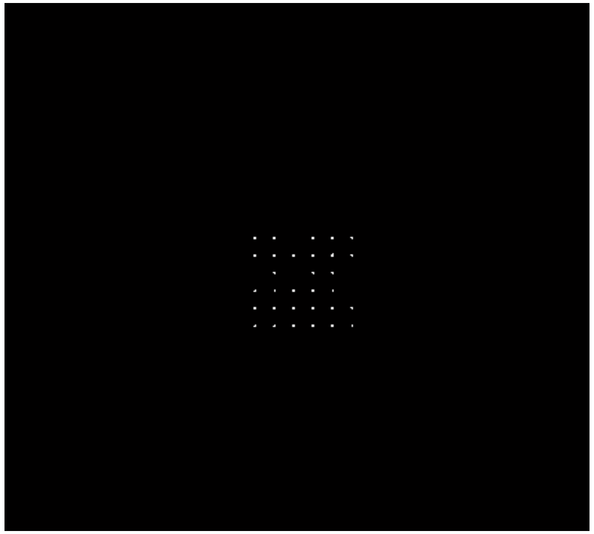

image with five sun spots missing

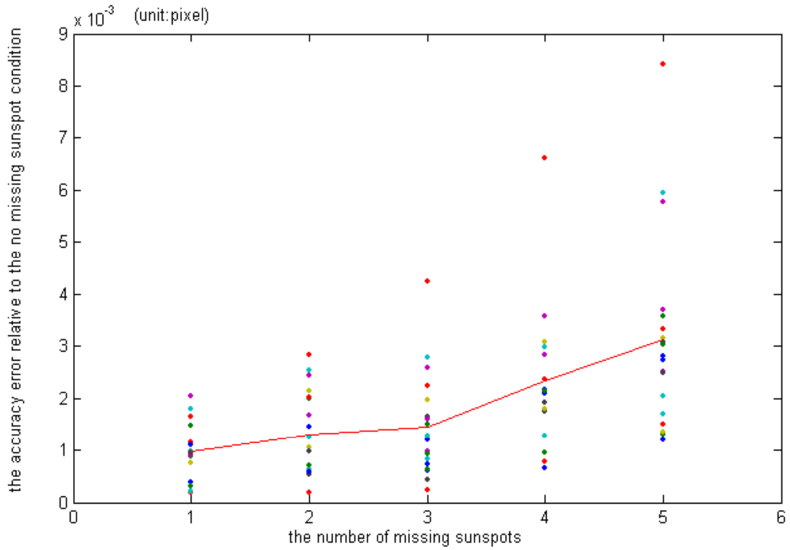

accuracy analysis with one–five sun spots missing at different sun angle of incidence.

➢conclusion

with five sun spots missing， the sun spots position error is no more than 0.01 pixels which is little effect on system accuracy.

Immunity performance(2)

2： image deteriorated

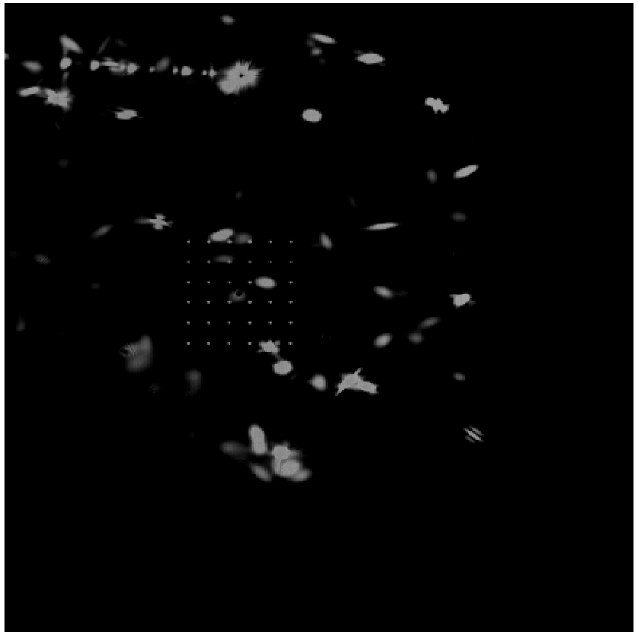

➢conclusion

Under above case, the sun sensor still works normally. It shows that the sun sensor has very strong immunity to image noise and harsh space environment.

System performance summary

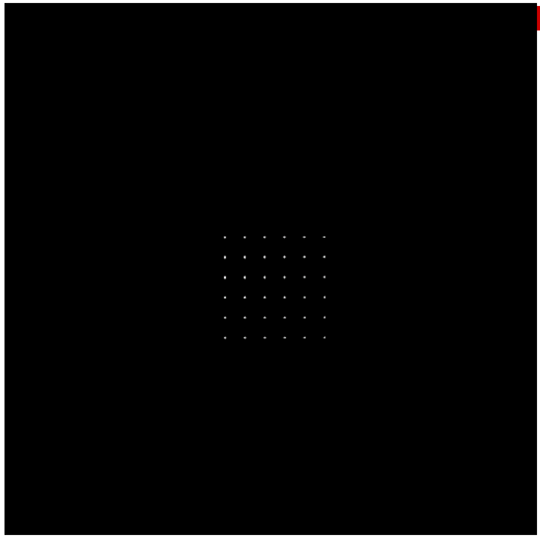

Normal case, 36 sun spots

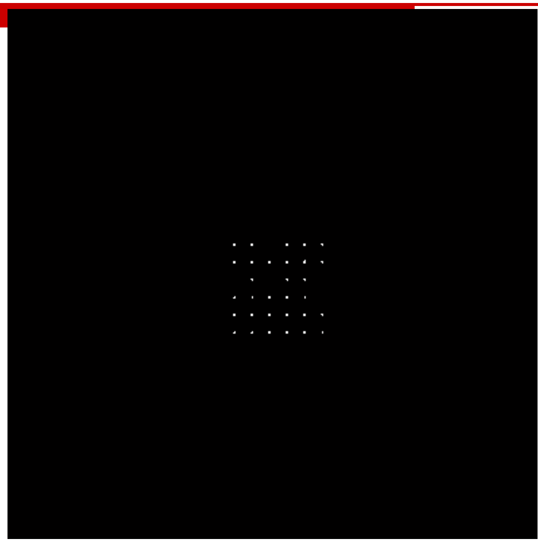

Some sun spots missing case

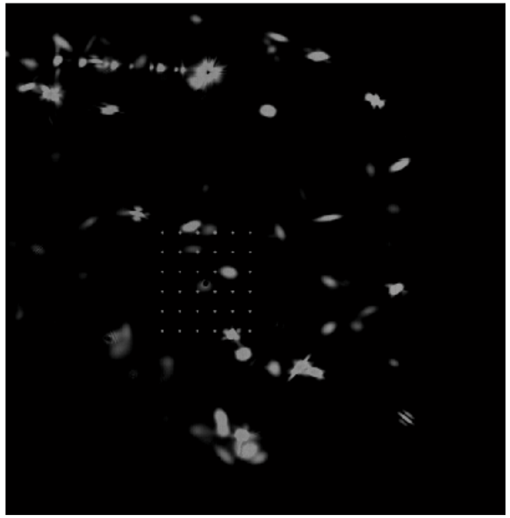

Image severely deteriorated case

① Normal case, system accuracy prior to 0.02 pixel

② Some sun spots missing case, keep same accuracy with ①

③ Image deteriorated case, keep system normally works.

Testing in Space

SY-3 satellite

MEMS sun sensor

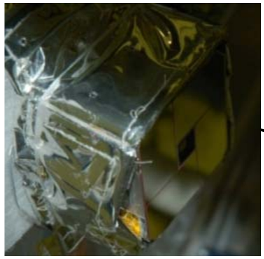

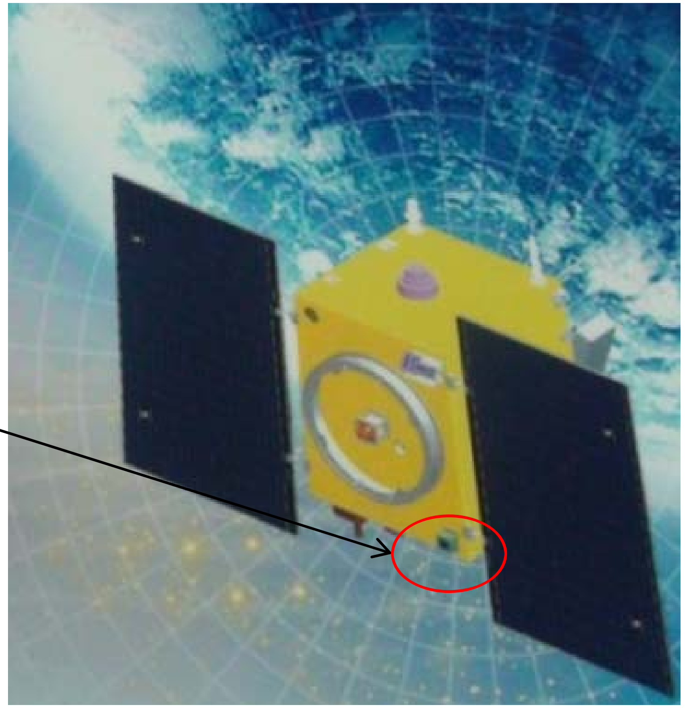

The SY-3 satellite with our MEMS sun sensor was launch in JiuQuan launch center of China, Nov.5,2008

Testing in Space

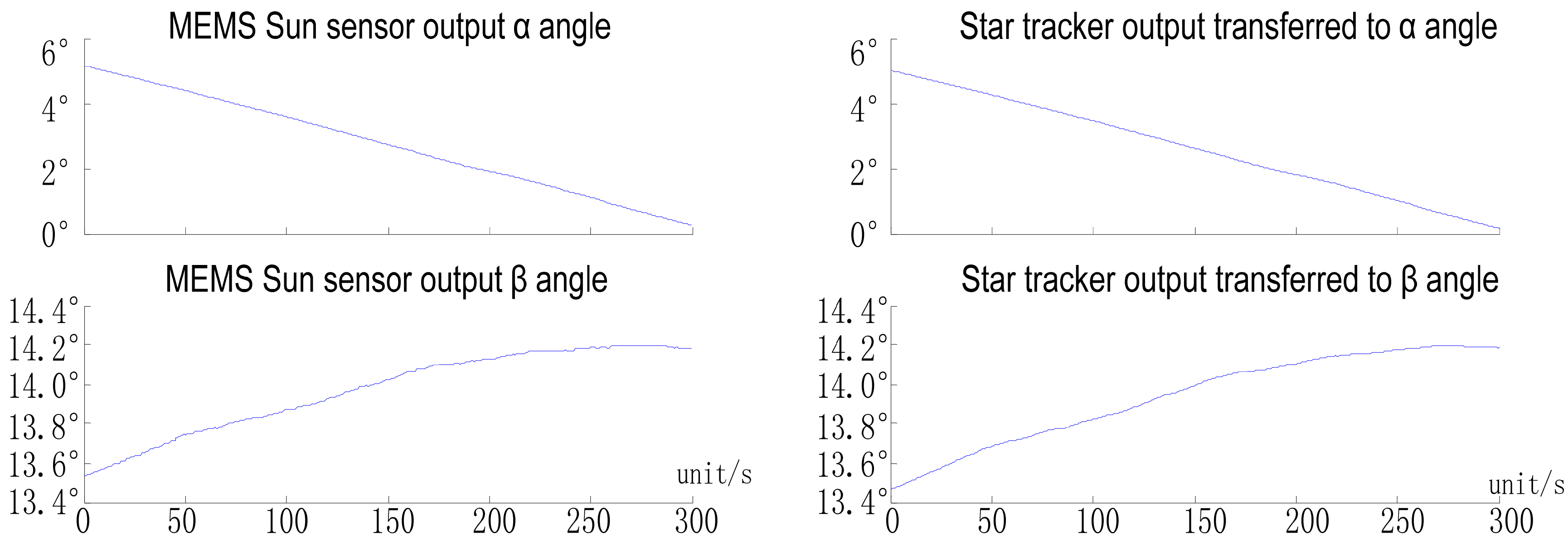

7:00~7:05, Nov. 12 ,2008

The comparing of MEMS sun sensor output result and the star tracker output result, that has been transfer to the sun sensor coordinate.

Testing in Space

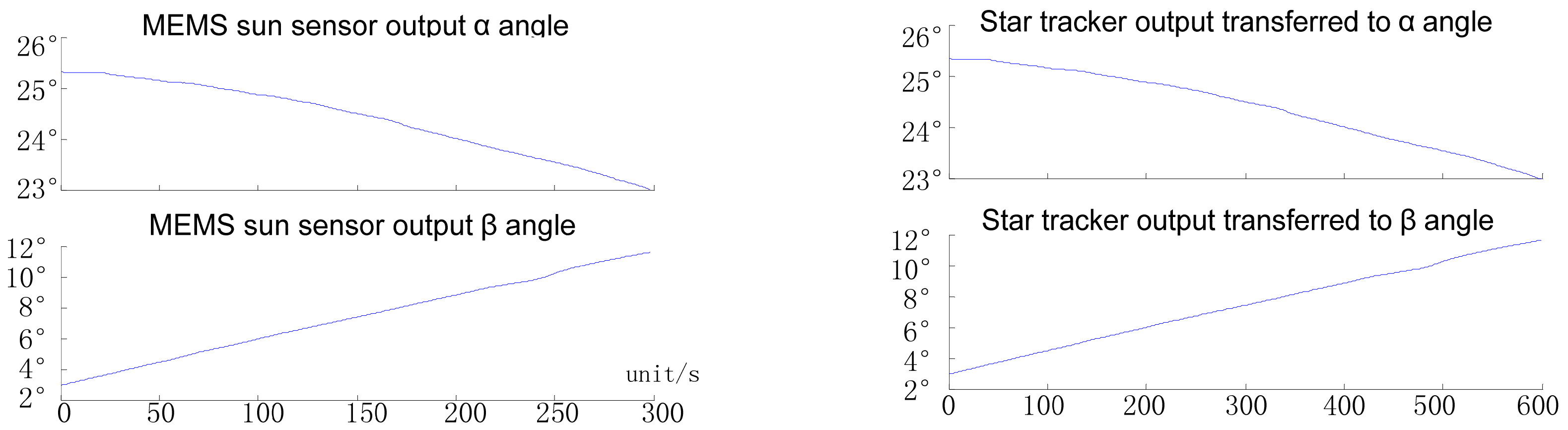

8:36~8:41, Aug. 7 ,2009

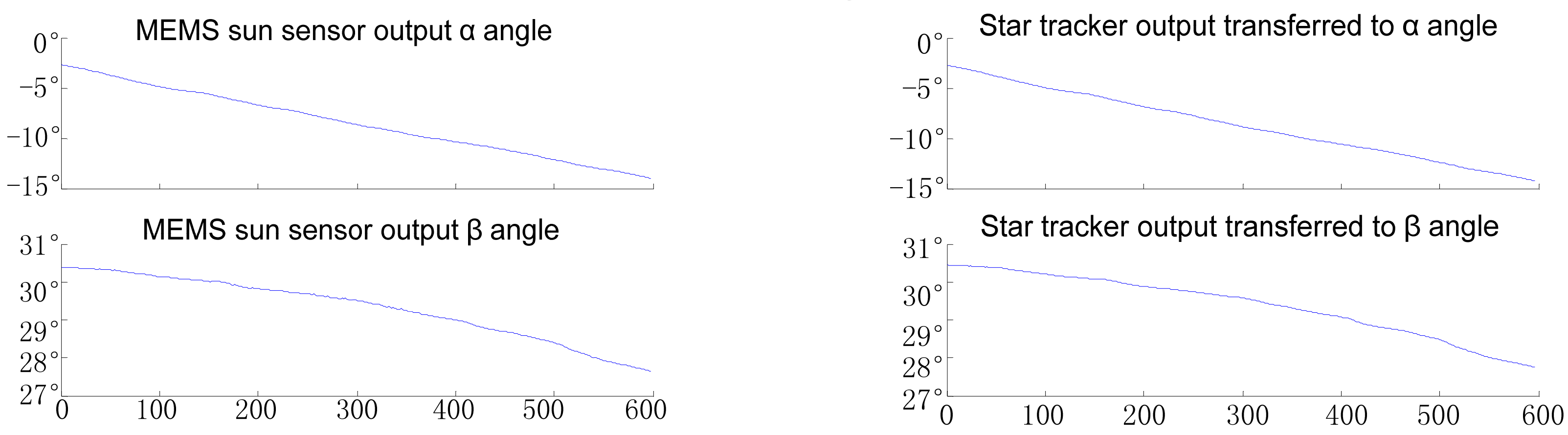

18:15~18:20, July. 8 ,2010

Accuracy Analysis

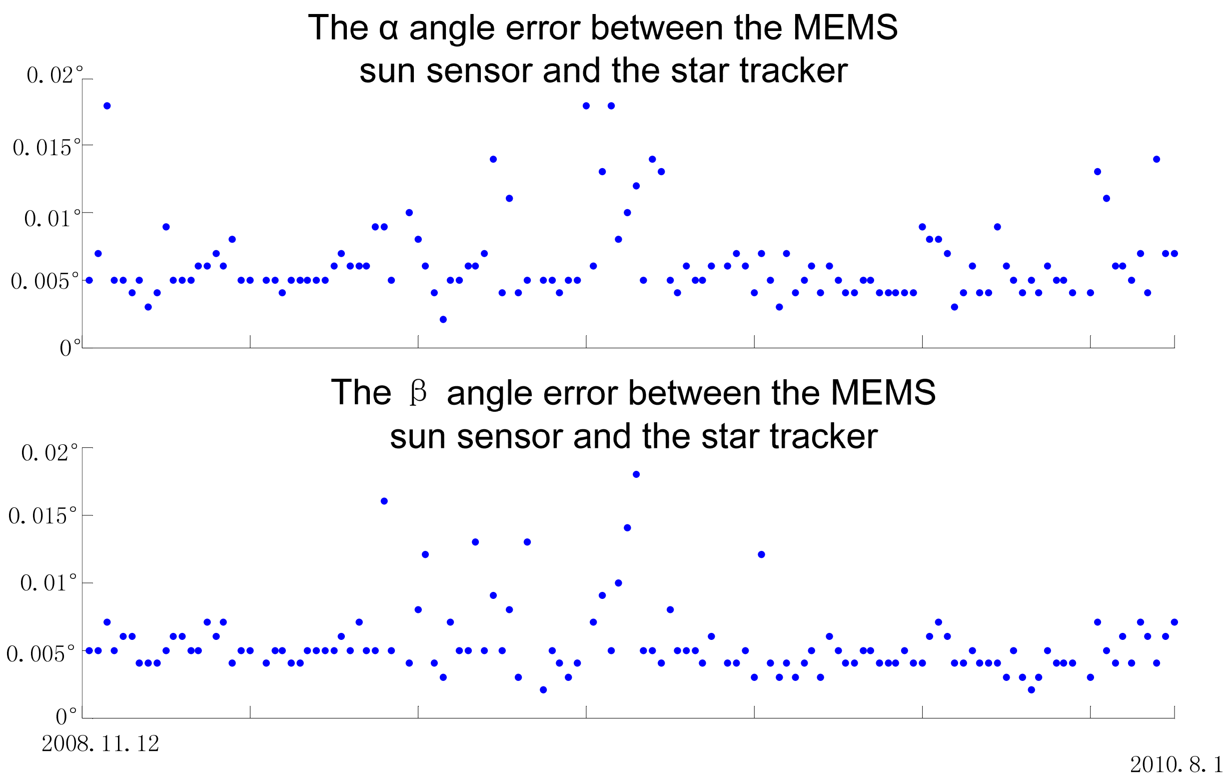

On orbit test, the accuracy of MEMS sun sensor is prior to 0.02° 。

Penumbra and eclipse test

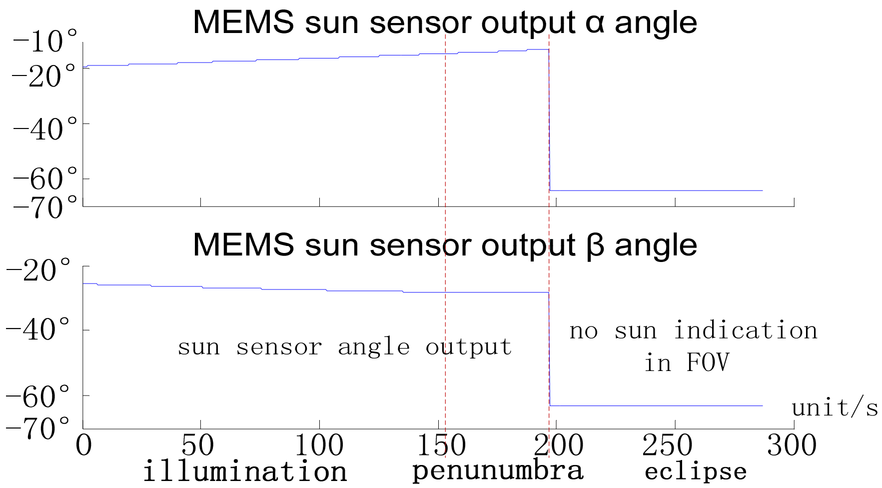

July 9 ,2009, 6:35~6:40, the satellite start the process from the sun illumination via penumbra to eclipse.

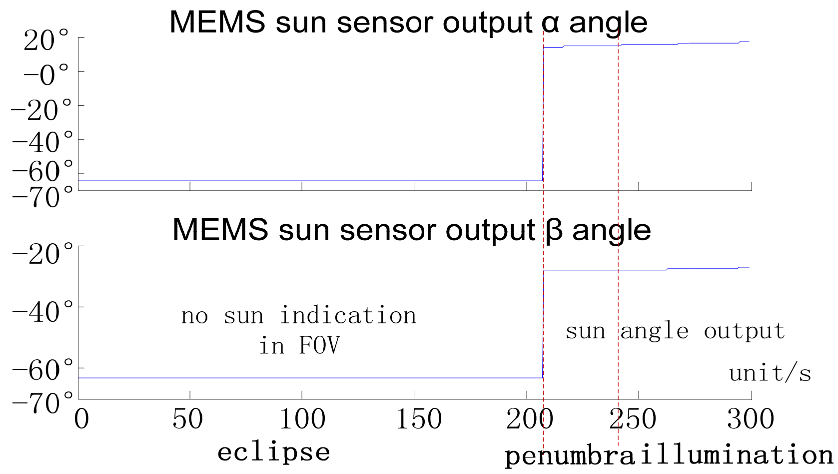

July 12 ,2009, 7:04~7:09, the satellite start the process from the eclipse via penumbra to illumination.

The experiment show the MEMS sun sensor can normally work on the process of the satellite into or out of the eclipse. 。

Contents

- **Introduction**
- **Engineering Model Construction**
- **FEIC algorithm**
- **Performance Validation on lab and orbit**
- **Summary**

Summary

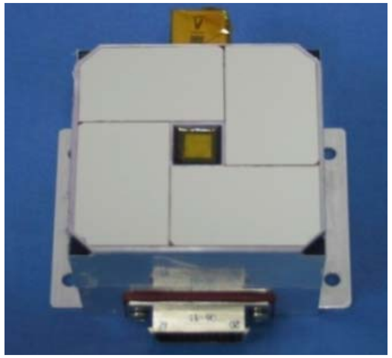

Tsinghua university-THU

（MEMS Sun Sensor）

parameter	THU MEMS Sun Sensor
accuracy	Prior to 0.02°
Field of View	128° ×128°
Resolution	Prior to 0.004°
mass	350g
Update data rate	10Hz

Summary

- **the MEMS based 36 apertures mark as the optical frond-end.**
- **Future extraction and image correlation-FEIC as the high accurate algorithm.**
- **Strong immune to some sun spots missing, image deteriorated and harsh space environment.**

Reference:

Fei Xing， Zheng You，GaoFei Zhang，Jian Sun. Anovel active pixels sensor (APS) based sun sensor based on a feature extraction and image correlation (FEIC) technique. ***Measurement Science &Technology*** **Vol: 19 Issue: 12 Pages: 125203 (9pp.) (SCI，UT ISI：000260759000007)。**

Contact: Xing Fei: xingfei@tsinghua.edu.cn;

Department of Precision Instruments and Mechanology, BLD 9003, RM2008,

Tsinghua University, BeiJing, China.